Blu-ray disk lens as the objective of a miniaturized two-photon fluorescence microscope

Hsiang-Yu Chung,[1,2] Wei-Cheng Kuo,[1] Yu-Hsiang Cheng,[1,2] Che-Hang Yu,[1] Shih-Hsuan Chia,[1] Cheng-Yung Lin,[3] Jie-Shin Chen,[3] Huai-Jen Tsai,[3] Andrey B. Fedotov,[4] Anatoly A. Ivanov,[4] Aleksei M. Zheltikov,[4] and Chi-Kuang Sun[1,2,5,6,*]

[1]Department of Electrical Engineering and Graduate Institute of Photonics and Optoelectronics, National Taiwan University, Taipei 10617, Taiwan
[2]Molecular Imaging Center, National Taiwan University, Taipei 10617, Taiwan
[3]Institute of Fisheries Science, National Taiwan University, Taipei 10617, Taiwan
[4]Department of Physics, International Laser Center, M.V. Lomonosov Moscow State University, Vorob'evy Gory, Moscow 119992, Russia
[5]Center for Optoelectronic Medicine & Graduate Institute of Biomedical Electronic and Bioinformatics, National Taiwan University, Taipei, 10617 Taiwan
[6]Institute of Physics & Research Center for Applied Sciences, Academia Sinica, Taipei 11529, Taiwan
[*]sun@ntu.edu.tw

Abstract: In this paper, we examine the performance of a Blu-ray disk (BD) aspheric lens as the objective of a miniaturized scanning nonlinear optical microscope. By combining a single 2D micro-electro mechanical system (MEMS) mirror as the scanner and with different tube lens pairs, the field of view (FOV) of the studied microscope varies from 59 μm × 93 μm up to 178 μm × 280 μm, while the corresponding lateral resolution varies from 0.6 μm to 2 μm for two-photon fluorescence (2PF) signals. With a 34/s video frame rate, *in vivo* dynamic observation of zebrafish heartbeat through 2PF of the excited green fluorescence protein (GFP) is demonstrated.

OCIS codes: (180.4315) Nonlinear microscopy; (190.4710) Optical nonlinearities in organic materials; (220.4830) Systems design.

References and links

1. W. Denk, J. H. Strickler, and W. W. Webb, "Two-photon laser scanning fluorescence microscopy," Science **248**(4951), 73–76 (1990).
2. I. Freund, M. Deutsch, and A. Sprecher, "Connective tissue polarity. Optical second-harmonic microscopy, crossed-beam summation, and small-angle scattering in rat-tail tendon," Biophys. J. **50**(4), 693–712 (1986).
3. D. Yelin and Y. Silberberg, "Laser scanning third-harmonic-generation microscopy in biology," Opt. Express **5**(8), 169–175 (1999).
4. T.-H. Tsai, C.-Y. Lin, H. J. Tsai, S. Y. Chen, S. P. Tai, K. H. Lin, and C.-K. Sun, "Biomolecular imaging based on far-red fluorescent protein with a high two-photon excitation action cross section," Opt. Lett. **31**(7), 930–932 (2006).
5. S.-Y. Chen, S.-U. Chen, H.-Y. Wu, W.-J. Lee, Y.-H. Liao, and C.-K. Sun, "In vivo virtual biopsy of human skin by using noninvasive higher harmonic generation microscopy," IEEE J. Sel. Top. Quantum Electron. **16**(3), 478–492 (2010).
6. M.-R. Tsai, S.-Y. Chen, D.-B. Shieh, P.-J. Lou, and C.-K. Sun, "In vivo optical virtual biopsy of human oral mucosa with harmonic generation microscopy," Biomed. Opt. Express **2**(8), 2317–2328 (2011).
7. J. C. Jung and M. J. Schnitzer, "Multiphoton endoscopy," Opt. Lett. **28**(11), 902–904 (2003).
8. J. C. Jung, A. D. Mehta, E. Aksay, R. Stepnoski, and M. J. Schnitzer, "In vivo mammalian brain imaging using one- and two-photon fluorescence microendoscopy," J. Neurophysiol. **92**(5), 3121–3133 (2004).
9. R. P. J. Barretto, B. Messerschmidt, and M. J. Schnitzer, "In vivo fluorescence imaging with high-resolution microlenses," Nat. Methods **6**(7), 511–512 (2009).
10. R. P. Barretto and M. J. Schnitzer, "In vivo optical microendoscopy for imaging cells lying deep within live tissue," in *Imaging: A Laboratory Manual* (Cold Spring Harbor Laboratory, 2011).
11. M. Chen, C. Xu, and W. W. Webb, "Endoscope lens with dual fields of view and resolutions for multiphoton imaging," Opt. Lett. **35**(16), 2735–2737 (2010).

#196680 - $15.00 USD Received 30 Aug 2013; revised 1 Nov 2013; accepted 2 Nov 2013; published 13 Dec 2013

12. F. Bortoletto, C. Bonoli, P. Panizzolo, C. D. Ciubotaru, and F. Mammano, "Multiphoton fluorescence microscopy with GRIN objective aberration correction by low order adaptive optics," PLoS ONE **6**(7), e22321 (2011).
13. T. A. Murray and M. J. Levene, "Singlet gradient index lens for deep in vivo multiphoton microscopy," J. Biomed. Opt. **17**(2), 021106 (2012).
14. J. Knittel, L. Schnieder, G. Buess, B. Messerschmidt, and T. Possner, "Endoscope-compatible confocal microscope using a gradient index-lens system," Opt. Commun. **188**(5–6), 267–273 (2001).
15. W. Göbel, J. N. D. Kerr, A. Nimmerjahn, and F. Helmchen, "Miniaturized two-photon microscope based on a flexible coherent fiber bundle and a gradient-index lens objective," Opt. Lett. **29**(21), 2521–2523 (2004).
16. B. A. Flusberg, J. C. Jung, E. D. Cocker, E. P. Anderson, and M. J. Schnitzer, "In vivo brain imaging using a portable 3.9 gram two-photon fluorescence microendoscope," Opt. Lett. **30**(17), 2272–2274 (2005).
17. R. Le Harzic, M. Weinigel, I. Riemann, K. König, and B. Messerschmidt, "Nonlinear optical endoscope based on a compact two axes piezo scanner and a miniature objective lens," Opt. Express **16**(25), 20588–20596 (2008).
18. R. Le Harzic, I. Riemann, M. Weinigel, K. König, and B. Messerschmidt, "Rigid and high-numerical-aperture two-photon fluorescence endoscope," Appl. Opt. **48**(18), 3396–3400 (2009).
19. C. J. Engelbrecht, R. S. Johnston, E. J. Seibel, and F. Helmchen, "Ultra-compact fiber-optic two-photon microscope for functional fluorescence imaging in vivo," Opt. Express **16**(8), 5556–5564 (2008).
20. D. R. Rivera, C. M. Brown, D. G. Ouzounov, I. Pavlova, D. Kobat, W. W. Webb, and C. Xu, "Compact and flexible raster scanning multiphoton endoscope capable of imaging unstained tissue," Proc. Natl. Acad. Sci. U. S. A. **108**(43), 17598–17603 (2011).
21. H. Bao, J. Allen, R. Pattie, R. Vance, and M. Gu, "Fast handheld two-photon fluorescence microendoscope with a 475 μm × 475 μm field of view for in vivo imaging," Opt. Lett. **33**(12), 1333–1335 (2008).
22. Y. Zhao, H. Nakamura, and R. J. Gordon, "Development of a versatile two-photon endoscope for biological imaging," Biomed. Opt. Express **1**(4), 1159–1172 (2010).
23. M. T. Myaing, D. J. MacDonald, and X. Li, "Fiber-optic scanning two-photon fluorescence endoscope," Opt. Lett. **31**(8), 1076–1078 (2006).
24. Y. Wu, Y. Leng, J. Xi, and X. Li, "Scanning all-fiber-optic endomicroscopy system for 3D nonlinear optical imaging of biological tissues," Opt. Express **17**(10), 7907–7915 (2009).
25. Y. Wu, J. Xi, M. J. Cobb, and X. Li, "Scanning fiber-optic nonlinear endomicroscopy with miniature aspherical compound lens and multimode fiber collector," Opt. Lett. **34**(7), 953–955 (2009).
26. Y. Wu, Y. Zhang, J. Xi, M.-J. Li, and X. Li, "Fiber-optic nonlinear endomicroscopy with focus scanning by using shape memory alloy actuation," J. Biomed. Opt. **15**(6), 060506 (2010).
27. K. Murari, Y. Zhang, S. Li, Y. Chen, M.-J. Li, and X. Li, "Compensation-free, all-fiber-optic, two-photon endomicroscopy at 1.55 μm," Opt. Lett. **36**(7), 1299–1301 (2011).
28. W. Liang, K. Murari, Y. Zhang, Y. Chen, M.-J. Li, and X. Li, "Increased illumination uniformity and reduced photodamage offered by the Lissajous scanning in fiber-optic two-photon endomicroscopy," J. Biomed. Opt. **17**(2), 021108 (2012).
29. J. Xi, Y. Chen, Y. Zhang, K. Murari, M.-J. Li, and X. Li, "Integrated multimodal endomicroscopy platform for simultaneous en face optical coherence and two-photon fluorescence imaging," Opt. Lett. **37**(3), 362–364 (2012).
30. Y. Zhang, K. Murari, W. Liang, J. Xi, Y. Chen, M.-J. Li, Z. Bhujwalla, K.Glunte, and X. Li, "Scanning nonlinear endomicroscopy technology for intrinsic imaging of biological tissues," in *CLEO: Applications and Technology*, paper ATh5A.1 (2012).
31. M. E. Fermann, "Single-mode excitation of multimode fibers with ultrashort pulses," Opt. Lett. **23**(1), 52–54 (1998).
32. D. G. Ouzounov, K. D. Moll, M. A. Foster, W. R. Zipfel, W. W. Webb, and A. L. Gaeta, "Delivery of nanojoule femtosecond pulses through large-core microstructured fibers," Opt. Lett. **27**(17), 1513–1515 (2002).
33. F. Helmchen, D. W. Tank, and W. Denk, "Enhanced two-photon excitation through optical fiber by single-mode propagation in a large core," Appl. Opt. **41**(15), 2930–2934 (2002).
34. W. Göbel, A. Nimmerjahn, and F. Helmchen, "Distortion-free delivery of nanojoule femtosecond pulses from a Ti:sapphire laser through a hollow-core photonic crystal fiber," Opt. Lett. **29**(11), 1285–1287 (2004).
35. C. L. Hoy, N. J. Durr, P. Chen, W. Piyawattanametha, H. Ra, O. Solgaard, and A. Ben-Yakar, "Miniaturized probe for femtosecond laser microsurgery and two-photon imaging," Opt. Express **16**(13), 9996–10005 (2008).
36. C. L. Hoy, O. Ferhanoğlu, M. Yildirim, W. Piyawattanametha, H. Ra, O. Solgaard, and A. Ben-Yakar, "Optical design and imaging performance testing of a 9.6-mm diameter femtosecond laser microsurgery probe," Opt. Express **19**(11), 10536–10552 (2011).
37. T.-M. Liu, M.-C. Chan, I.-H. Chen, S.-H. Chia, and C.-K. Sun, "Miniaturized multiphoton microscope with a 24Hz frame-rate," Opt. Express **16**(14), 10501–10506 (2008).
38. S.-H. Chia, C.-H. Yu, C.-H. Lin, N.-C. Cheng, T.-M. Liu, M.-C. Chan, I.-H. Chen, and C.-K. Sun, "Miniaturized video-rate epi-third-harmonic-generation fiber-microscope," Opt. Express **18**(16), 17382–17391 (2010).
39. E. D. Cocker, R. P. J. Barretto, J. C. Jung, B. A. Flusberg, H. Ra, O. Solgaard, and M. J. Schnitzer, "A portable two-photon fluorescence microendoscope based on a two-dimensional scanning mirror," in *Optical MEMS and Nanophotonics, 2007 IEEE/LEOS International Conference*, 6–7 (2007).
40. W. Piyawattanametha, E. D. Cocker, L. D. Burns, R. P. J. Barretto, J. C. Jung, H. Ra, O. Solgaard, and M. J. Schnitzer, "In vivo brain imaging using a portable 2.9 g two-photon microscope based on a microelectromechanical systems scanning mirror," Opt. Lett. **34**(15), 2309–2311 (2009).
41. L. Fu, A. Jain, H. Xie, C. Cranfield, and M. Gu, "Nonlinear optical endoscopy based on a double-clad photonic crystal fiber and a MEMS mirror," Opt. Express **14**(3), 1027–1032 (2006).

#196680 - $15.00 USD Received 30 Aug 2013; revised 1 Nov 2013; accepted 2 Nov 2013; published 13 Dec 2013

42. L. Fu, A. Jain, C. Cranfield, H. Xie, and M. Gu, "Three-dimensional nonlinear optical endoscopy," J. Biomed. Opt. **12**(4), 040501 (2007).
43. W. Jung, S. Tang, D. T. McCormic, T. Xie, Y.-C. Ahn, J. Su, I. V. Tomov, T. B. Krasieva, B. J. Tromberg, and Z. Chen, "Miniaturized probe based on a microelectromechanical system mirror for multiphoton microscopy," Opt. Lett. **33**(12), 1324–1326 (2008).
44. S. Tang, W. Jung, D. McCormick, T. Xie, J. Su, Y.-C. Ahn, B. J. Tromberg, and Z. Chen, "Design and implementation of fiber-based multiphoton endoscopy with microelectromechanical systems scanning," J. Biomed. Opt. **14**(3), 034005 (2009).
45. http://panasonic.net/blu-ray/technology/story01/
46. G. F. Marshall and G. E. Stutz, *Handbook of Optical and Laser Scanning*, 2nd ed. (CRC, 2012).
47. J. B. Pawley, *Handbook of Biological Confocal Microscopy*, 3rd ed. (Springer, 2006).
48. S.-P. Tai, M.-C. Chan, T.-H. Tsai, S.-H. Guol, L.-J. Chen, and C.-K. Sun, "Two-photon fluorescence microscope with a hollow-core photonic crystal fiber," Opt. Express **12**(25), 6122–6128 (2004).
49. S. W. Smith, *The Scientist and Engineer's Guide to Digital Signal Processing* (California Technical, 1997).
50. M. Offroy, Y. Roggo, and L. Duponchel, "Increasing the spatial resolution of near infrared chemical images (NIR-CI): The super-resolution paradigm applied to pharmaceutical products," Chemom. Intell. Lab. Syst. **117**, 183–188 (2012).
51. R. F. Fischer and B. Tadic, *Optical System Design* (McGtaw-Hill, 2000).
52. D. C. Brown, "Decentering distortion of lenses," Photogramm. Eng. **32**(3), 444–462 (1966).
53. J. P. de Villiers, F. W. Leuschner, and R. Geldenhuys, "Centi-pixel accurate real-time inverse distortion correction," in *International Symposium on Optomechatronic Technologies*, SPIE (2008).
54. C.-Y. Lin, P.-H. Yang, C.-L. Kao, H.-I. Huang, and H.-J. Tsai, "Transgenic zebrafish eggs containing bactericidal peptide is a novel food supplement enhancing resistance to pathogenic infection of fish," Fish Shellfish Immunol. **28**(3), 419–427 (2010).
55. C.-J. Huang, C.-T. Tu, C.-D. Hsiao, F.-J. Hsieh, and H.-J. Tsai, "Germ-line transmission of a myocardium-specific GFP transgene reveals critical regulatory elements in the cardiac myosin light chain 2 promoter of zebrafish," Dev. Dyn. **228**(1), 30–40 (2003).
56. E. Spiess, F. Bestvater, A. Heckel-Pompey, K. Toth, M. Hacker, G. Stobrawa, T. Feurer, C. Wotzlaw, U. Berchner-Pfannschmidt, T. Porwol, and H. Acker, "Two-photon excitation and emission spectra of the green fluorescent protein variants ECFP, EGFP and EYFP," J. Microsc. **217**(3), 200–204 (2005).
57. M. Westerfield, *The Zebrafish Book*, 3rd ed. (University of Oregon, 1995).

1. Introduction

Nonlinear optical microscopies, such as two-photon fluorescence (2PF) microscopy [1] or harmonic generation (HG) microscopy [2–6] are useful techniques for biomedical imaging. Due to the nature of optical nonlinearity, they possess high viability, deep penetration, and fine optical sectioning capability without using a pinhole in comparison with the confocal microscopy. A nonlinear optical microscope system is typically composed of three parts: a pulsed laser light source, the optical microscope components (including mirrors and lenses), and the scanning module. Unlike the traditional wide-field optical microscope, an additional scanner is usually needed for a nonlinear optical microscope in order to scan the focused laser beam over the FOV, which makes the whole system bulkier. As a result and for future intravital applications, many groups have worked on the miniaturization of the system [7–44] in recent ten years.

The effort of the miniaturization can also be divided to three parts: laser sources, optical components, and the scanners. In this study we focus on the study of the miniaturization of the objective, or more specifically, we focus on the study of the potential of the current widely available blu-ray disk (BD) lens as the objective of the nonlinear scanning microscope. By combining a single 2D micro-electro mechanical system (MEMS) mirror as the scanner and with different commercially available tube lens pairs, the field of view (FOV) of the studied microscope can vary from 59 μm × 93 μm up to 178 μm × 280 μm, while the corresponding lateral resolution varies from 0.6 μm to 2 μm for two-photon fluorescence (2PF) signals, comparable to or better than previously reported miniaturized 2PF microscope by using a GRIN rod as the objective. With a high 34/s video frame rate, *in vivo* observation of zebrafish heartbeat is demonstrated by two-photon excitation of green fluorescence protein (GFP) with a 920 nm light.

#196680 - $15.00 USD Received 30 Aug 2013; revised 1 Nov 2013; accepted 2 Nov 2013; published 13 Dec 2013

2. Miniaturized system and experimental methods

2.1 Miniaturized imaging head

The latest Blu-ray disk technology uses a 405 nm blue light as the light source and a 0.85 NA lens as the optical reader which provides a 25 GB data storage capacity [45]. This high NA lens is used in the optical disk drive and is designed for normal incident light. In order to apply the nonlinear optical microscopy for clinical applications, microscope systems with a miniaturized size, a large FOV, and a high frame rate is strongly desired. A large FOV means that we can reveal more information simultaneously. The high frame rate cannot only solve the image blurring problem resulted from inevitable vibrations during the observation, but also allow one to reduce the imaging acquisition time, while dynamic observation can be realized. Considering these demands, we construct the miniaturization system by integration of a 2D MEMS scanner with the studied BD lens. Only the most critical components are included in this study, so we have only 5 lenses or mirrors inside the whole imaging head. Those components are chosen due to their small-size with a diameter within several millimeters to centimeters and their easy availability with a low-cost. They include a MEMS mirror as the scanning module, a BD lens as the objective, a tube lens pair for beam size magnification, and a dichroic beam splitter to separate the excitation light and the collected 2PF signal.

2.1.1 MEMS scanning mirror

The two-dimensional (2D) scanning MEMS mirror (PE100011, OPUS) (Fig. 1) can provide high frequency resonant scanning to achieve high frame rates as previously reported [35–38,40]. Considering both the scanning efficiency and the missing pixel problem, we decided to set the scanning frequency of the fast axis to be 16.02 kHz and the slow axis to be 1.75 kHz. With such a high scanning speed, the frame rate can reach up to 34/s without missing pixels. The clear diameter of the scanning mirror itself is only 1.2 mm. To avoid power loss, a pair of telescope was used to adjust the excitation beam size to just cover the scanning mirror. However, since the MEMS mirror is 45° oblique to the excitation light, the effective cross-sectional area is smaller than its physical size. The reflected beam became elliptic with a longer axis of 1.2 mm diameter and a shorter axis of $1.2\times\frac{1}{\sqrt{2}}\cong 0.84$ mm diameter. Therefore, beam size magnification is needed considering the clear aperture of the BD lens.

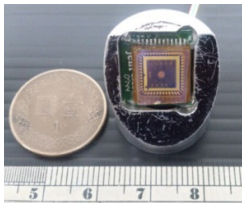

Fig. 1. The mounted MEMS scanning mirror chip. The mirror is the tiny round object in the very center.

2.1.2 Mini aspheric lens

Aspheric lenses are known for their complicated surface profile designed for spherical aberration reduction or replacement of a multi-lens system. In comparison with the GRIN (gradient-index) lens, they have relatively higher NA and suffer less chromatic aberration. They're widely used in 3C products, such as: camera of cellular phones, optical disk drives, and video players. They're also used for laser diode collimation and light coupling of optical fibers. Their size are small within several millimeters, thus we choose them as the objective lens. The BD lens (Panasonic) we used is an aspheric lens with 0.85 NA. It's directly

#196680 - $15.00 USD Received 30 Aug 2013; revised 1 Nov 2013; accepted 2 Nov 2013; published 13 Dec 2013

dismounted from a laptop-used optical drive. The lens is plastic. Since there are no detailed specs of the lens, we simply measure it by a ruler. It is 2.5 mm long in diameter and 1.5 mm in thickness. The clear aperture of the lens is about 2 mm. The lens is originally designed for the 405 nm blue light, so the transmission for the 920 nm infrared we used as the excitation source is only 50%. The transmission for green light is about 70% measured by using a 532 nm laser pointer as the light source.

2.1.3 Tube lens pair

A tube lens pair, which is composed of a scan lens and a tube lens, is aligned between the MEMS scanning mirror and the aspheric objective lens. As the MEMS mirror rotates, the collimated incidence will pass through the scan lens and the tube lens with different angles. After passing through the tube lens, the resulted beams become collimated again and scan across the back focal plane of the objective lens [46,47]. With different ratios of the beam size magnification, the tube lens pair controls how much the clear aperture (CA) as well as the scanning angle onto the objective will be covered. In other words, it serves as an imaging system to image the scanner onto the objective back aperture, which controls the laser incident angle (and thus the field of view) into the objective. We designed three different tube lens pairs for beam size magnification experiment (Fig. 2): the 1:1 magnification, the 1:1.5 magnification, and the 1:3 magnification. The different combinations of the BD lens and the tube lens pair provide various kinds of FOV and resolution.

The 1:3 tube lens pair is composed of two commercial plano-convex spherical lens (KPX010AR.16, KPX016AR.16, Newport) to cover 100% CA of the BD lens, thus providing a better resolution but a smaller FOV. The 1:1.5 tube lens pair (KPX013AR.16, KPX016AR.16, Newport) covers only 2/3 of the CA which has a larger FOV. The 1:1 tube lens covers less than half of the CA but provides the largest FOV. The design of the 1:1 tube lens pair was carried out by the optical design program ZEMAX, and it is composed of two home-made biconvex spherical lenses fabricated by ITRC (Instrument Technology Research Center, Taiwan). The ZEMAX parameters designed for the home-made biconvex spherical lenses and the simulated result of the optical path difference (OPD) by using the home-made tube lens pair are shown in Fig. 3 and Fig. 4, respectively.

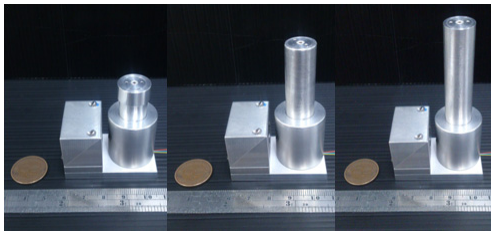

Fig. 2. Replaceable tube lens pairs mounted with the packaged system with magnification ratio 1:1, 1:3, and 1:1.5 (from left to right). A dichroic beam splitter is mounted in the left square mount in order to separate the excitation light and the collected 2PF signal. The cylinder on the right is composed of a replaceable tube lens pair and the MEMS scanning unit.

	Surf:Type	Comment	Radius	Thickness		Glass		Semi-Diameter	
OBJ	Standard		Infinity	Infinity				Infinity	
STO	Standard		Infinity	5.000000				0.420000	U
2*	Standard		9.860948	5.000000		SF11		5.000000	U
3*	Standard		-8.170207	10.000000				5.000000	U
4*	Standard		10.903525	7.000000		SF11		5.000000	U
5*	Standard		-8.832714	5.000000				5.000000	U
6*	Paraxial			0.700000	V			1.000000	U
IMA	Standard		Infinity	-				0.109944	

Fig. 3. The ZEMAX design parameters of the 1:1 home-made tube lens pair with the BD lens.

#196680 - $15.00 USD Received 30 Aug 2013; revised 1 Nov 2013; accepted 2 Nov 2013; published 13 Dec 2013

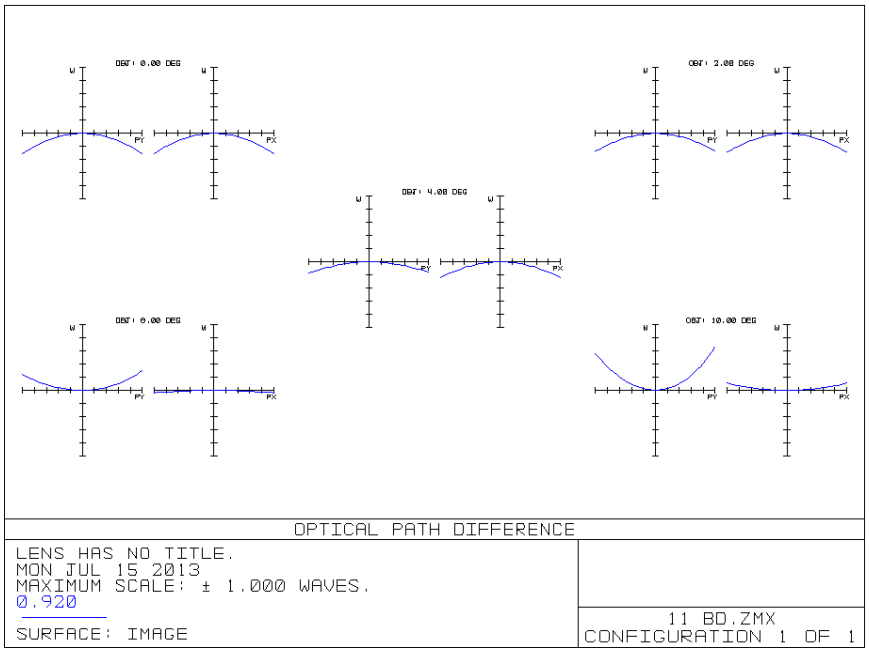

Fig. 4. The simulated result by ZEMAX showing the optical path difference (OPD) of the 1:1 tube lens pair with the substitute of the BD lens. The figure has 5 groups, which correspond to incidences from 5 different incident angles (0°, 2°, 4°, 8°, 10°). Each group has two graphs, which are the OPD in x and in y directions respectively. The test wavelength is 0.920 μm, and the result indicates the maximum wavefront difference is smaller than λ/2, so the resolution won't be affected much by the oblique incidence.

2.2 Electronic control and instant data processing

Since the scanning speed of the MEMS mirror is 16.02 kHz in fast axis and 1.75 kHz in slow axis, the sampling rate must be even higher during the scanning. Sampling frequency up to 36.7 MHz is needed to ensure every pixel of a 512 × 512 pixel frame will be captured with a 34/s frame rate.

With such a high sampling frequency, a tremendous amount of data will be generated, so mass data acquisition and instant mapping become crucial tasks. A PXIe computer system (NI PXIe-1082, NI PXIe-8133, NI 8260, National Instruments) with a FPGA card (NI 5761, National Instruments) for data acquisition is introduced to deal with this problem. It is capable of instant data acquisition and mapping in 2-channel 14-bit 512 × 512 pixels frame. With a 1 TB RAID (redundant array of independent disks), the data can be recorded continuously for two hours.

The electronic control core of the system is another commercial FPGA card (DE2, Altera). It can generate 4 electronic control signals. Two of them are the fast axis and the slow axis signals to drive the MEMS mirror. The other two are the sampling frequency and the frame trigger for the PXIe system. With all 4 signals synchronized, a real-time continuous video image can be shown on the monitor while the experiment is conducted.

3. Experimental setup

Figure 5 is the free-space setup of the experiment. We use a Ti: Sapphire pulsed laser (Mira 900, Coherent) as the excitation source. The excitation wavelength is 920 nm. The red line indicates the excitation light. First, a telescope (L1 + L2) (KPX112, KPX094, Newport) was used to adjust the laser beam size to match the MEMS scanning mirror. Next, the excitation light enters the imaging head system and passes through a DBS (dichroic beam splitter) (FF705-Di01, Semrock). Due to the coating, it only allows infrared light to pass, but reflects

#196680 - $15.00 USD Received 30 Aug 2013; revised 1 Nov 2013; accepted 2 Nov 2013; published 13 Dec 2013

the visible light. After passing through the beam splitter, the excitation light will be reflected by the MEMS mirror and pass through the tube lens pair (L3 + L4) and the aspheric objective lens (L5). While it reaches the sample, nonlinear optical signal will be generated. The green light indicates the epi-collected 2PF signal. It traces back almost through the same path but will be reflected by the DBS and enters a PMT (photomultiplier tube) (R4220P, Hamamatsu). A band pass filter (BPF) (FF01-520.35-25) was set to filter the green fluorescence signal. It is important to notice that in this study, we only report the result for free-space incident light. However, fiber collimators can be directly mounted to the system for fiber-based light source [38,48] or nonlinear signal delivery [38], as shown in Fig. 6.

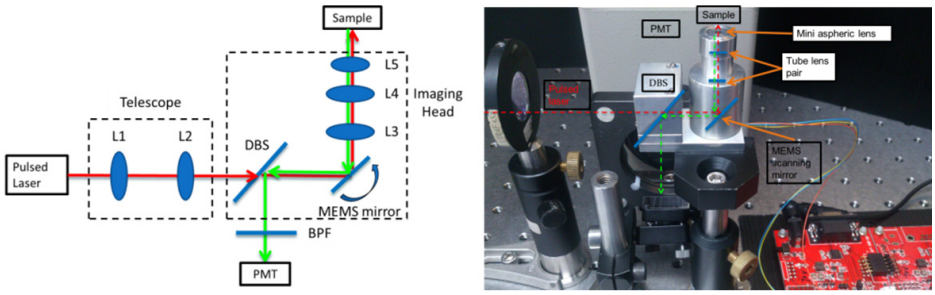

Fig. 5. Free-space setup of the experiment.

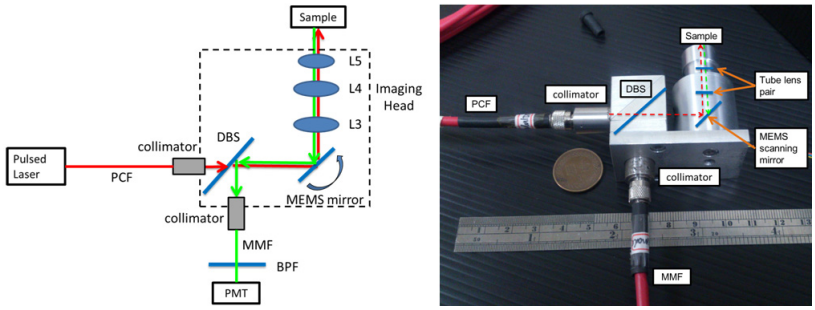

Fig. 6. Fiber-based setup of the experiment. The setup is similar to Fig. 5. Collimators can be directly mounted to the system for fiber-based light source or signal collection delivery. Photonic crystal fibers (PCF) could be used to deliver the light from the bulk laser source to the imaging head to prevent the pulse distortion, whereas multi-mode fibers (MMF) could be used for the delivery of the collected signal.

4. Performance

4.1 Field of view (FOV) estimation

We use the green fluorescent dye of a common highlighter (WKP1-G, ZEBRA, Japan) to dye the 1951 USAF resolution test chart (#59-152, Edmund) to analyze the FOV and the resolution of our system. By comparing the length of the rulings in the image, we can estimate the actual area of the FOV (Fig. 7). For double confirmation, we also move the resolution test chart by using a high-precision delay stage for FOV estimation.

#196680 - $15.00 USD Received 30 Aug 2013; revised 1 Nov 2013; accepted 2 Nov 2013; published 13 Dec 2013

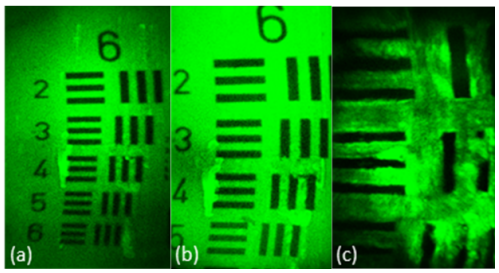

Fig. 7. The FOV of the 2PF microscope by using the BD lens as the objective with different tube lens pairs. (a) FOV: 178 μm × 280 μm with the 1:1 tube lens pair. (b) FOV: 121 μm × 200 μm with the 1:1.5 tube lens pair. (c) FOV: 59 μm × 93 μm with the 1:3 tube lens.

4.2 Resolution estimation

Here we use the "step-edge" method [49] to estimate the lateral resolution. Considering a "step-edge" source as the input of the optical system, then the actual acquired signal is the edge response. We can get the line spread function (LSF) in the considered direction by differentiating the edge response with respect to the position. Finally, the full width at half maximum (FWHM) is regarded as the estimation of the lateral resolution [50].

To evaluate the resolution from different part of the figure, we divided the figure into 4 pieces and assumed the resolution in each quadrant is similar due to the symmetry. Then we randomly chose one quadrant and divided it into a 3 × 3 area to analyze the resolution. Different values of the resolution from those areas are expected since we consider that the oblique incidence onto the BD lens would lead to aberrations. Table 1 summarizes our result.

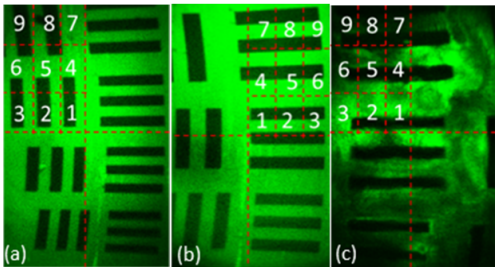

Fig. 8. Sample pictures for resolution analysis of the 2PF microscope by using the BD lens with (a) the 1:1, (b) the 1:1.5, and (c) the 1:3 tube lens pairs. First, each figure was divided into 4 pieces. Then one of the quadrants was further divided into a 3 × 3 area and labeled from 1 to 9. Due to oblique incidence, we expect a difference of the resolution between the central part of the imaging area (ex: area 1, area 2, or area 4) and the marginal part of the imaging area (ex: area 3, area 7, or area 9).

Table 1. Image resolution from different imaging area of the BD lens-based 2PF microscope with different tube lens pairs. (unit: μm)

Tube lens	Area	1	2	3	4	5	6	7	8	9
1:1	x-direction	1.63	1.73	1.85	1.76	1.89	1.99	1.93	2.03	2.09
	y-direction	1.66	1.76	1.82	1.78	1.86	1.98	1.95	2.00	2.08
1:1.5	x-direction	1.06	1.12	1.16	1.13	1.21	1.21	1.19	1.22	1.26
	y-direction	1.04	1.13	1.18	1.18	1.22	1.24	1.20	1.27	1.29
1:3	x-direction	0.60	0.63	0.66	0.64	0.67	0.75	0.69	0.77	0.80
	y-direction	0.62	0.64	0.70	0.67	0.71	0.77	0.72	0.78	0.79

#196680 - $15.00 USD Received 30 Aug 2013; revised 1 Nov 2013; accepted 2 Nov 2013; published 13 Dec 2013

4.3 Distortion aberration

In Fig. 8, the shape of the rulings starts to distort as the FOV increased. This effect is called "distortion" [51], which is one kind of optical aberration. It is originated from the difference of the transverse magnification of a lens. The two most common distortions are the positive and the negative distortions. They're also called "pincushion" or "barrel" due to the deformed shapes. The distortion could be corrected and simulated by a Brown's distortion model [52].

Due to the fact that distortion is primarily dominated by the low order radial components [53], we post-processed the collected images to correct the distortion using ImageJ and PhotoImpact by correcting the first and second order radial distortion coefficients, while those corrected values can be found by using the acquired images from the 1951 USAF resolution test chart.

4.4 Two-photon fluorescence (2PF) sample images

We used the green fluorescence protein (GFP) zebrafish (*Danio rerio*) and the micro-fluorescent-beads (F-13081, Life Technologies) to double-check the performance of BD lens-based 2PF microscopy. Tissue specific and ubiquitous promoter drives *gfp* as the promoter gene expressing in different parts of the zebrafish, such as: whole body [54] or heart [55]. The peak 2PF excitation wavelength for GFP is at 920 nm [56], and the emission wavelength peak is at 520 nm [56]. For the micro fluorescent beads, we also use the 920 nm light as the excitation wavelength, and its emission wavelength peak is located between 505 and 515 nm. Figure 9 shows the 2PF images of the zebrafish with *gfp* as the promoter gene expressing in the whole body. The FOV of each image is 178 μm × 280 μm observed with the 1:1 tube lens pair and with the BD lens as the objective lens. By stitching 4 or 5 images together we can clearly recognize the head or the body part of the fish. To demonstrate the sub-micron resolution power, the 2PF image of the green micro-fluorescent-beads observed by the BD lens with the 1:3 tube lens pair is shown in Fig. 10. The beads are 1μm wide in diameter, and the FOV is 59 μm × 93 μm.

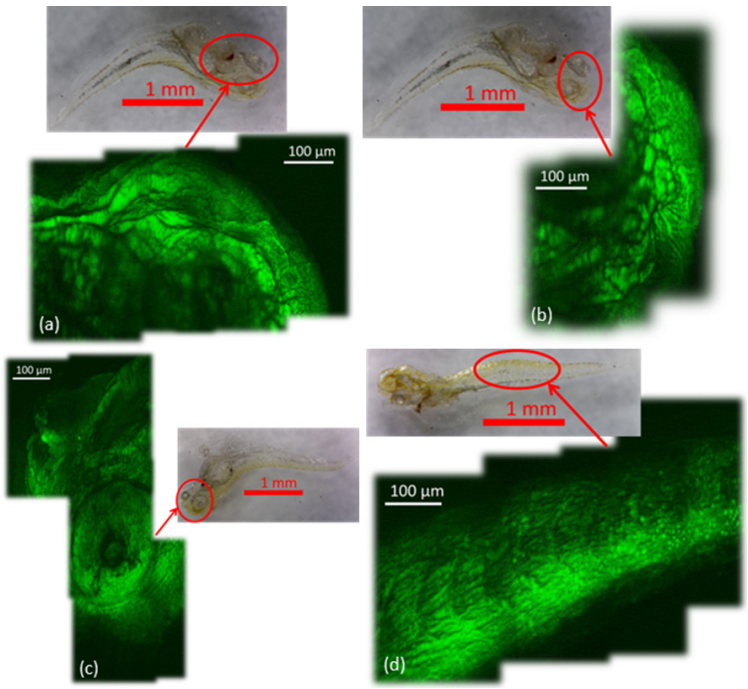

Fig. 9. 2PF images of GFP zebrafish (BD lens with the 1:1 tube lens pair). (a) and (b) Head of the fish. (c) Eyes of the fish. (d) Body of the fish. The fish were all 96 hpf (hours post fertilization). The FOV of each image is 178 μm × 280 μm before being stitched together.

#196680 - $15.00 USD Received 30 Aug 2013; revised 1 Nov 2013; accepted 2 Nov 2013; published 13 Dec 2013

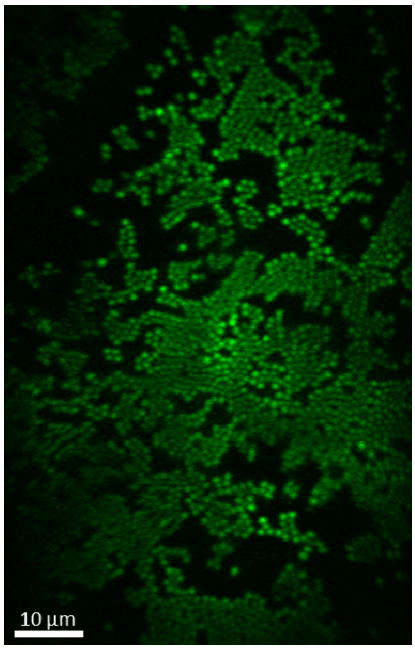

Fig. 10. The acquired 2PF image of 1 μm-diameter green fluorescent beads, clearly resolving individual beads with a sub-micron resolution. (BD lens with the 1:3 tube lens pair) FOV: 59 μm × 93 μm.

4.4 Real-time in vivo zebrafish heartbeat observation

Our study indicates that the developed 2PF microscope with a miniaturized size is not only with a high spatial resolution, but also provides a high imaging frame rate, thus enabling real-time *in vivo* dynamic observation. To test this capability, we applied our BD-lens-based 2PF microscope for zebrafish heart beat observation.

The fish juvenile we used were 72 hpf (hours post fertilization), and the tissue specific promoter drives *gfp* as the reporter gene expressing in the heart of zebrafish [55]. Thus, we can observe the atrium and the ventricle structures composed of the GFP myocardium cells. For imaging, first, the fish was anesthetized by tricane (3-amino benzoic acid ethyl ester). It would stop the movement of the fish, but keeps its heartbeat. The heart rate may be lowered, but the dose is not harmful to the fish [57]. Then we used the agarose gel to mount the fish on a microslide [57]. Figure 11 shows the time-sequenced images of the heat beat acquired with our miniaturized 2PF microscope with a 34Hz frame rate. 1:1 tube lens pair was adopted with the BD lens as the objective. We can easily find that the heart was composed of two parts. The upper part showing the cell nuclei is the atria, and the lower part is the ventricle. Through high-speed imaging, we can see the atrium contracting while the ventricle expanding, and vice versa. The observed heart rate was around 180/min.

#196680 - $15.00 USD Received 30 Aug 2013; revised 1 Nov 2013; accepted 2 Nov 2013; published 13 Dec 2013

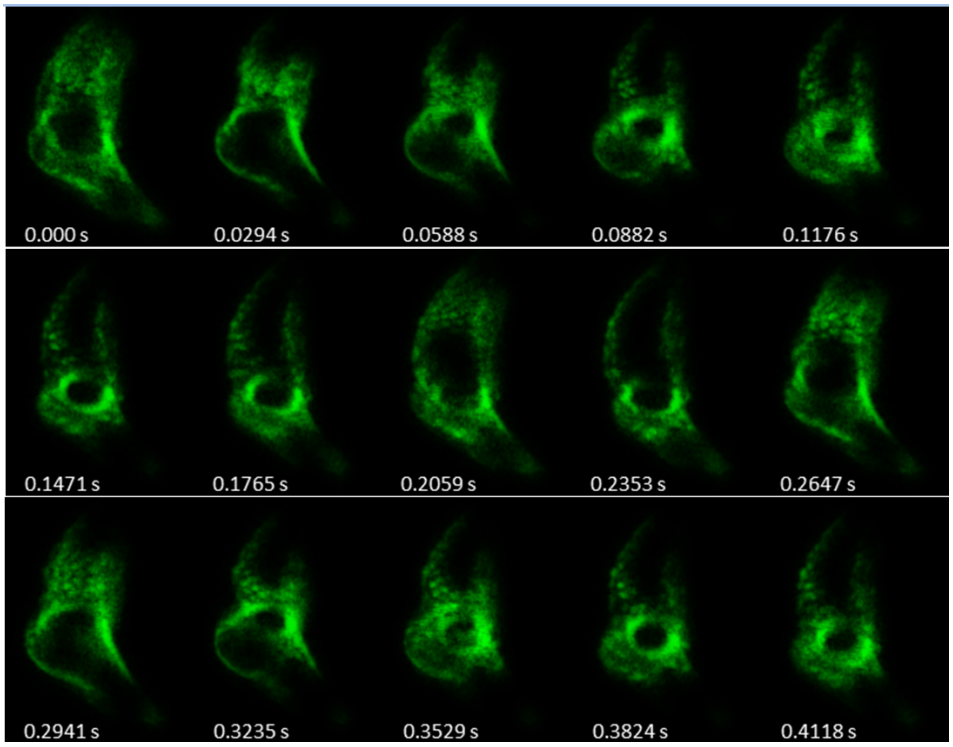

Fig. 11. Time lapse image sequence of the heartbeat of the zebrafish with myocardium GFP (BD lens with the 1:1 tube lens pair) from the lateral view. With a 34/s frame rate, the time interval between each image is about 0.0294 s. FOV: 178 μm × 280 μm. The attached file (Media 1) is an 11 s video. For the first 3 seconds, the observation depth was kept the same. Then we slightly adjusted the depth deeper to observe different parts of the heart with a rate of 100 μm/s.

5. Summary

In this work, a miniaturized two-photon fluorescence microscope based on a 0.85 NA BD objective lens and a MEMS scanning mirror is demonstrated. FOV from 59 μm × 93 μm up to 178 μm × 280 μm is realized by simply changing different tube lens pairs. By combining the BD lens with the a commercially available spherical tube lens pair, 0.60 micron lateral resolution is achieved and is comparable or much better than most of the previous work [7–44]. Fast scanning and high speed data acquisition with a video frame rate is demonstrated. The heartbeat of a GFP zebrafish is successfully observed which suggests our miniaturized system is capable of being applied to the observation of various *in vivo* dynamic biological activities.

Acknowledgments

This project is sponsored by the National Science Council of Taiwan under grant numbers of NSC 100-2923-E-002-006-MY3 and the National Health Research Institute under grant numbers of NHRI-EX102-9936EI.

#196680 - $15.00 USD Received 30 Aug 2013; revised 1 Nov 2013; accepted 2 Nov 2013; published 13 Dec 2013